

The Role of Interocean Exchanges on Decadal Variations of the Meridional Heat Transport in the South Atlantic

SHENFU DONG

CIMAS, University of Miami, and NOAA/AOML, Miami, Florida

SILVIA GARZOLI AND MOLLY BARINGER

Physical Oceanography Division, NOAA/AOML, Miami, Florida

(Manuscript received 6 August 2010, in final form 19 April 2011)

ABSTRACT

The interocean exchange of water from the South Atlantic with the Pacific and Indian Oceans is examined using the output from the ocean general circulation model for the Earth Simulator (OFES) during the period 1980–2006. The main objective of this paper is to investigate the role of the interocean exchanges in the variability of the Atlantic meridional overturning circulation (AMOC) and its associated meridional heat transport (MHT) in the South Atlantic. The meridional heat transport from OFES shows a similar response to AMOC variations to that derived from observations: a 1 Sv ($1 \text{ Sv} \equiv 10^6 \text{ m}^3 \text{ s}^{-1}$) increase in the AMOC strength would cause a 0.054 ± 0.003 PW increase in MHT at approximately 34°S . The main feature in the AMOC and MHT across 34°S is their increasing trends during the period 1980–93. Separating the transports into boundary currents and ocean interior regions indicates that the increase in transport comes from the ocean interior region, suggesting that it is important to monitor the ocean interior region to capture changes in the AMOC and MHT on decadal to longer time scales. The linear increase in the MHT from 1980 to 1993 is due to the increase in advective heat converged into the South Atlantic from the Pacific and Indian Oceans. Of the total increase in the heat convergence, about two-thirds is contributed by the Indian Ocean through the Agulhas Current system, suggesting that the warm-water route from the Indian Ocean plays a more important role in the northward-flowing water in the upper branch of the AMOC at 34°S during the study period.

1. Introduction

In the Atlantic, one of the most prominent ocean circulation systems is the Atlantic meridional overturning circulation (AMOC), which is characterized by a northward flow of warm water in the upper layers from the tropics and the South Atlantic into the North Atlantic and a southward return flow of cold water at depth (e.g., Broecker 1991; Lumpkin and Speer 2007). In recent years, great interest in the AMOC has been aroused because of its link to past abrupt climate change and anthropogenic climate forcing (e.g., Broecker 1997; Stocker and Schmittner 1997; Gregory et al. 2005). The majority of efforts made to understand the driving mechanism of the AMOC and its variability have, to date, been focused

on the North Atlantic. However, the South Atlantic is particularly important as a region where oceanic properties are exchanged, mixed, and redistributed between different ocean basins beyond the Atlantic itself (e.g., Gordon 1985; Saunders and King 1995; Biastoch et al. 2008). This water mass exchange, modification, and redistribution process in the South Atlantic can significantly alter long-term AMOC response and therefore impact global climate (Weijer et al. 1999, 2002; Sloyan and Rintoul 2001; Sarmiento 2004; Marsh et al. 2007; Garzoli and Matano 2011).

Many processes are involved in the meridional overturning circulation in the South Atlantic (Fig. 1), including the interocean exchanges with the Pacific and Indian Oceans. The circulation pattern in the South Atlantic makes it unique as the only major ocean basin that transports heat from the poles toward the equator (e.g., Talley 2003). The net heat transport from the South Atlantic to the North Atlantic depends on the ratio of the water mass contributions from the south Indian Ocean and from the

Corresponding author address: Shenfu Dong, CIMAS, University of Miami and NOAA/AOML, 4301 Rickenbacker Causeway, Miami, FL 33149.
E-mail: shenfu.dong@noaa.gov

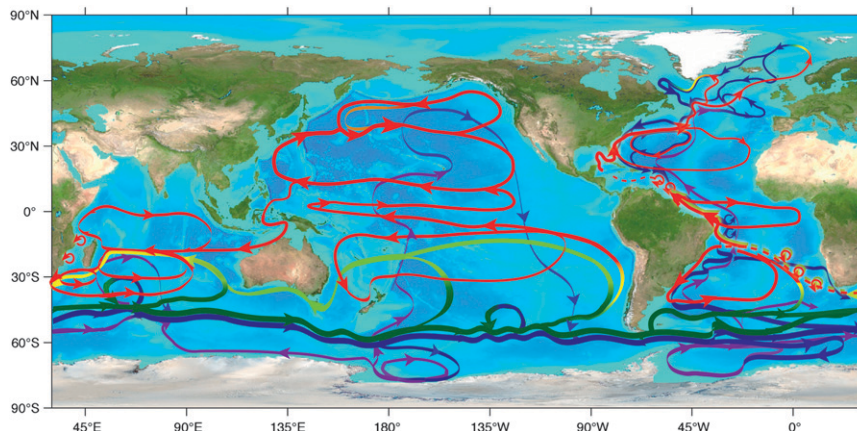


FIG. 1. Schematic diagram of the global ocean overturning circulation that represents the large-scale conversion of surface waters (red arrows) to deep waters (blue and purple arrows). Yellow and green arrows represent transitions between depths. Adapted from R. Lumpkin (2010, personal communication) and modified by S. Speich (2010, personal communication).

South Pacific Ocean (Garzoli and Gordon 1996). However, there is still some debate about whether the water transported to the north in the upper layer of the AMOC comes from the Pacific through the Drake Passage (e.g., Rintoul 1991) or from the Indian Ocean through the Agulhas retroflection region (e.g., Gordon 1985), although the latter possibility has garnered more support in recent years. The meridional heat transport (MHT) may also depend on how much heat the ocean gained from the atmosphere and how much heat is stored in the ocean. Thus, to understand the changes of the heat transported to the north in the South Atlantic on seasonal to longer time scales, it is important to determine the variability in the interocean exchanges and its underlying mechanism, as well as the variations in heat storage and air–sea heat fluxes. A better understanding of the interocean exchanges and thermal balance in the South Atlantic may potentially improve our ability to predict long-term climate change because of its link to the AMOC.

It has been recognized that there is a need to develop and enhance sustained observing systems to monitor meridional mass and heat transports to advance our knowledge of the long-term variability in AMOC and its climate impact. Despite the importance of the South Atlantic, the majority observations are focused on the North Atlantic: for example, the Rapid Climate Change (RAPID)/Meridional Overturning Circulation Heat-flux Array (MOCHA) program at 26.5°N (e.g., Cunningham et al. 2007). One compilation of existing monitoring programs for the AMOC can be found online (at <http://www.atlanticmoc.org/>) and is described in Cunningham et al. (2010). The only existing repeated transbasin observation in the subtropical South Atlantic is a high-density transbasin expendable bathythermograph (XBT) line at

nominal 34°S (Baringer and Garzoli 2007; Garzoli and Baringer 2007). However, no observational record is presently long enough to examine variability in the AMOC and its associated heat transport on decadal to longer time scales.

In this study, the outputs from an eddy-resolving ocean general circulation model are analyzed with an aim to gain more understanding of the longer-term variability in the processes related to AMOC in the South Atlantic. The basic information of the model simulation used in this study is described in section 2. In section 3, the volume and heat transports across 34°S (the northern boundary of our study region) and the interocean exchanges with the Pacific and Indian Oceans are estimated and analyzed. Our analyses are focused on the role of interocean exchanges in the long-term variations of the MHT across 34°S. Discussion and conclusions are given in section 4.

2. Model

The analysis in this study is based on a multidecadal hindcast by the global ocean general circulation model for the Earth Simulator (OFES). The model code is based on the third version of the Modular Ocean Model (MOM3; Pacanowski and Griffies 1999) and has been modified for optimal performance by the Earth Simulator Center of Japan. OFES covers the global domain from 75°S to 75°N with an eddy-resolving horizontal resolution of 0.1° and 54 vertical levels, with layer thickness increasing from 5 m at the surface to 330 m near the ocean bottom. The model was first spun up for 50 yr from an initial condition at rest with observed mean temperature/salinity fields from *World Ocean Atlas 1998* (WOA98) and monthly climatological atmospheric forcing from the National Centers

for Environmental Prediction–National Center for Atmospheric Research (NCEP–NCAR) reanalysis, which was followed by a 57-yr hindcast run for the period of 1950–2006 using the NCEP–NCAR reanalysis daily-mean surface forcing data. Readers are directed to Nonaka et al. (2006) and Sasaki et al. (2007) for detailed description of OFES. The OFES hindcast simulation is highly realistic in a broad range of variability on various time scales (e.g., Maximenko et al. 2005; Sasaki et al. 2007), and it has been widely used to investigate various climate problems (e.g., Nonaka et al. 2006; Taguchi et al. 2007; von Storch et al. 2007). Most of these studies are focused on the Pacific Ocean; to date, few studies have examined its performance in the South Atlantic. A recent study by E. Giarolla and R. P. Matano (2011, personal communication) found that, in the South Atlantic, OFES reproduces well the variability of the large-scale circulation, although it underestimates the quasi-decadal increasing trend of the sea surface height (SSH) observed from altimetry. Perez et al. (2011) suggested that the western boundary current is better represented in OFES in terms of its zonal and vertical structure compared to some other models. The surface eddy kinetic energy (EKE) from OFES well captures the high EKE in the Brazil–Malvinas confluence and Agulhas Current system regions, as compared to the EKE derived from altimetry (Fig. 2). However, OFES is too energetic in the boundary current regions, and the Agulhas rings prefer a northward corridor with pathways not as diverse as is seen in altimetry (Fig. 2).

The current analysis is limited to the period 1980–2006, when the OFES outputs are readily available. The model outputs have been decimated to $0.2^\circ \times 0.2^\circ$ and 3-day averages. Our analyses for the 27-yr model outputs are focused on a region in the South Atlantic bounded by 34°S to the north and by 65°W and 20°E to the west and east, respectively. The southern boundary of the study region is bounded by 75°S , the southern boundary of the model (Fig. 2). The northern boundary is chosen to approximately collocate with an existing transbasin XBT line (Baringer and Garzoli 2007) for comparison with available estimates of the AMOC strength and meridional heat transport.

The model captures well the major current systems in our study region (Fig. 3), including the northward-flowing Benguela Current at the eastern boundary; its extension to form the northern boundary of the subtropical gyre; and the westward-flowing Agulhas Current south of South Africa, which retroflects and returns eastward around $38^\circ\text{--}40^\circ\text{S}$. At the western boundary, the southward-flowing Brazil Current, the northward-flowing Malvinas Current, and the Brazil–Malvinas Confluence at $\sim 38^\circ\text{S}$ where the two currents meet are all well

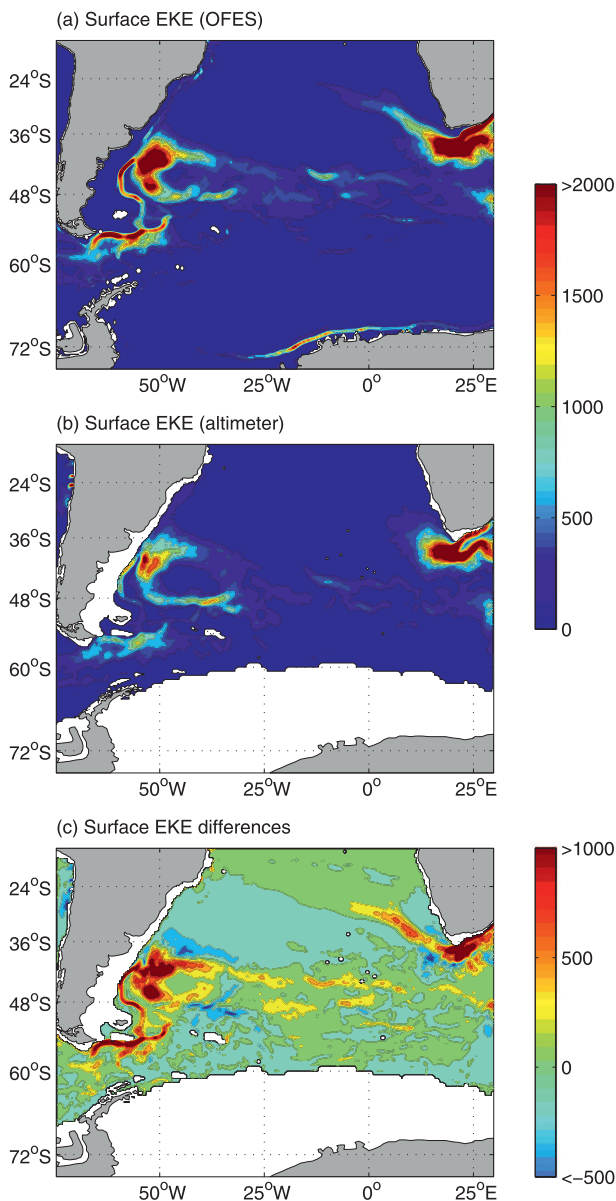


FIG. 2. Time-mean EKE at the ocean surface computed from the geostrophic velocity of (a) OFES and (b) satellite altimetry. (c) The differences between (a) and (b). Units are $\text{cm}^2 \text{s}^{-2}$.

represented in the model. The model also captures the Antarctic Circumpolar Current (ACC) and the Weddell gyre in the Southern Ocean. All these major features of the currents in our study region compare well with the current structure derived from the satellite-based mean SSH (Fig. 3b). Note that the mean SSH is a combination of Gravity Recovery and Climate Experiment (GRACE) mission, altimetry, and in situ data (Rio and Hernandez 2004). The mean velocity from the model is stronger than that from the observed SSH, particularly in the boundary

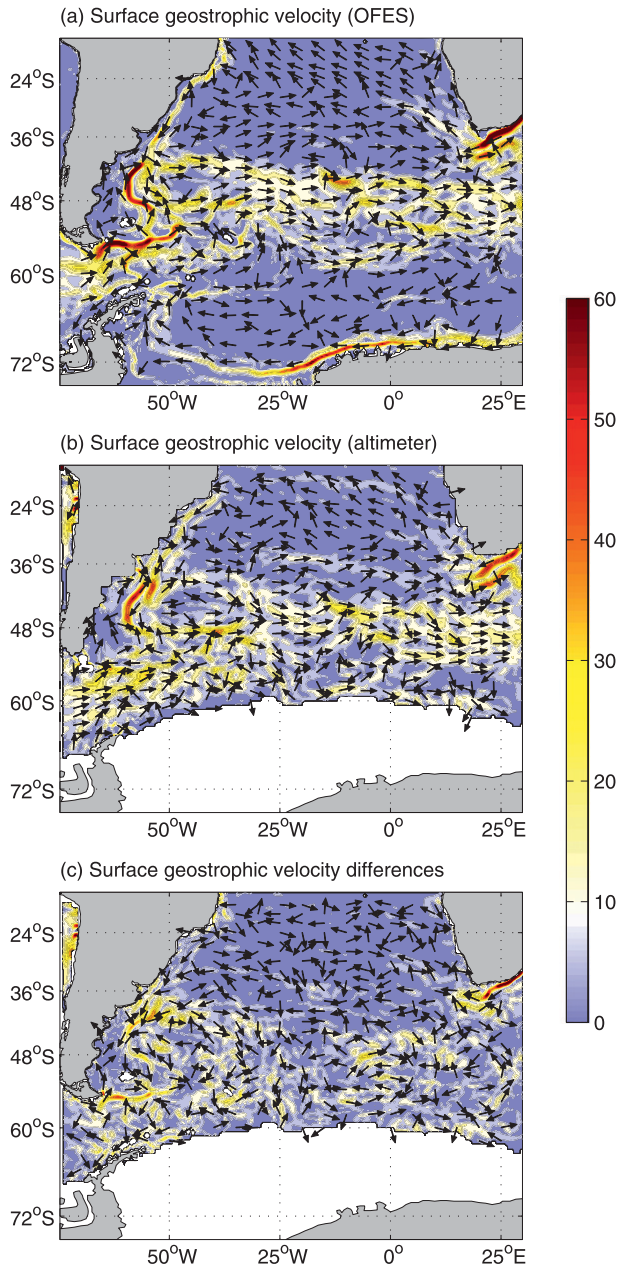


FIG. 3. Time-mean geostrophic velocity fields at ocean surface derived from (a) OFES modeled sea level and (b) the mean SSH from a combination of GRACE mission, altimetry, and in situ data. (c) The differences between (a) and (b). Color shading indicates the speed of the currents in cm s^{-1} , and the current direction is shown as the arrows.

current regions, such as the Agulhas Current off the South Africa coast.

Volume and heat transports across each boundary are calculated from the OFES velocity and temperature fields to examine the variations in the MHT at 34°S and its relationship with interocean exchanges and the variations in the AMOC. To assess the contributions of geostrophic

and Ekman transports to changes in volume and heat transports across each boundary, we estimate the Ekman transport using the wind stress and sea surface temperature from the model. No statistically significant changes were found when the temperature at upper 50 m is used to estimate Ekman transport. The geostrophic transport is estimated as the difference between the total transport and the Ekman component. Note that, using OFES, Perez et al. (2011) found that the sum of the geostrophic and Ekman transports reproduces well the total transports, suggesting that the bottom Ekman layer effect is small.

It should be noted that it is appropriate to use the terminology of heat transport at 34°S , where the volume transport is close to zero, as well as when the sum of transport in our study region is considered because of the mass conservation in a fixed region. However, it is inappropriate to use heat transport for the eastern and western boundaries due to large net volume transport. However, because our analyses are in the context of the fixed region, we use heat transport throughout the paper for consistency. Another way to understand this is that heat transport can be defined with a reference temperature. In our case, heat transport is computed with reference temperature of 0°C . The heat transport is computed as $\int \rho C_p \theta v dx dz$, where θ is potential temperature; v is meridional velocity; and ρ and C_p are the density and specific heat of seawater, respectively. The vertical axis is denoted by z and zonal (northern boundary) or meridional (western and eastern boundaries) axis by x . Space- and time-varying ρ and C_p , derived from OFES temperature and salinity fields, are used in heat transport calculation; using fixed values for ρ and C_p will not change our results significantly.

3. Results from OFES

In this section, we first calculate the time-mean volume and heat transports across each boundary, as well as the mean strength of the AMOC at 34°S . Then, we focus on the temporal variations of those transports on longer time scales and their potential causes.

a. Time mean

1) VOLUME AND HEAT TRANSPORTS

To illustrate the mean circulation structure and what comes in and out of the South Atlantic, we show the 27-yr-averaged vertically integrated volume transport and the corresponding total transport across each boundary in Fig. 4a. The major components of the transport across 34°S come from the boundary currents: the northward-flowing Benguela Current at the eastern boundary and

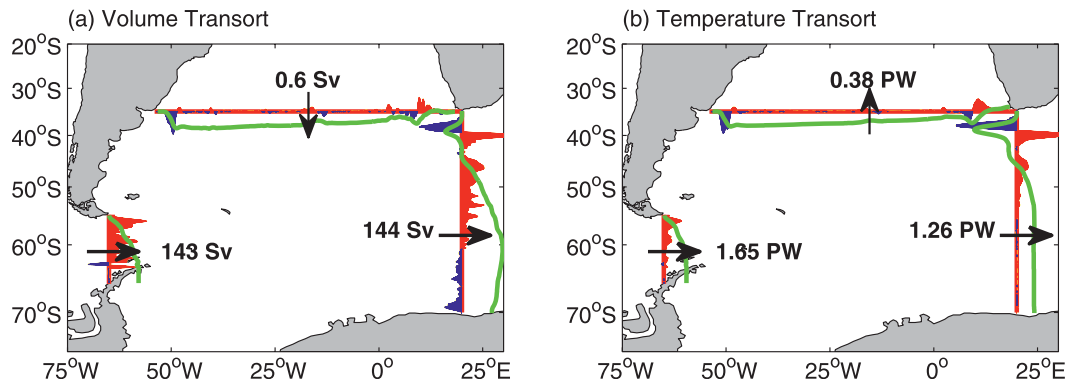


FIG. 4. Time-mean (a) volume and (b) heat transport across each boundary of our study region in the South Atlantic. The red/black shading indicates the vertically integrated transport at each location. The green lines show the cumulative transports from west to east for the northern boundary and from north to south for the western and eastern boundaries. The direction and value of total transport across each boundary are given by the arrows and numbers.

the southward-flowing Brazil Current and deep western boundary current at the western boundary. The net volume transport across 34°S is southward but very small, about -0.6 Sv ($1\text{ Sv} \equiv 10^6\text{ m}^3\text{ s}^{-1}$), with a standard deviation of 1.3 Sv , consistent with previous estimates from hydrographic data and inverse models (Baringer and Garzoli 2007; Lumpkin and Speer 2007; Dong et al. 2009). The southward transport across 34°S is coherent with the Bering Strait transport of OFES, which has a mean of 0.6 Sv (H. Sasaki 2010, personal communication). The transport across Drake Passage is dominated by the eastward-flowing ACC. The net eastward transport across 65°W is $143 \pm 5\text{ Sv}$ on average, close to previous estimates using hydrographic measurements [e.g., $134 \pm 11\text{ Sv}$ (Whitworth et al. 1982), $140 \pm 6\text{ Sv}$ (Ganachaud and Wunsch 2000), $137 \pm 8\text{ Sv}$ (Cunningham et al. 2003)]. Unlike the ACC-dominant transport across Drake Passage, there are two major current systems south of South Africa: the eastward-flowing ACC and the westward-flowing Agulhas Current and its return flow. However, the net eastward transport across 20°E is similar to that across Drake Passage, $144 \pm 5\text{ Sv}$, which is expected for volume conservation.

The heat transport across each boundary is shown in Fig. 4b. The 27-yr mean heat transport across 34°S is about $0.38 \pm 0.23\text{ PW}$ ($1\text{ PW} = 10^{15}\text{ W}$) to the north, lower than the 0.54 PW derived from XBT measurements (Dong et al. 2009; Garzoli and Baringer 2007). This weak heat transport is likely due to the weak AMOC strength from OFES [see section 3a(2) for further discussion]. The total heat transport includes two components: the geostrophic and Ekman transports. The Ekman transport accounts for $0.14 \pm 0.17\text{ PW}$, which is consistent with Dong et al. (2009). The contribution from geostrophic flow, $0.24 \pm 0.13\text{ PW}$, is lower than the value of 0.4 PW

derived from XBT measurements (Dong et al. 2009). Thus, the weak total heat transport across 34°S is due to the weak geostrophic transport in the model [see also section 3a(2)].

The meridional heat transport can be divided into three components: the barotropic, overturning (baroclinic), and the horizontal heat fluxes. Readers are directed to Bryden and Imawaki (2001) for detailed description of the methodology. In short, both meridional velocity and potential temperature are separated into three components: section-averaged values ($\langle \underline{v} \rangle$, $\langle \underline{\theta} \rangle$), zonally averaged baroclinic values [$\langle \underline{v} \rangle(z)$, $\langle \underline{\theta} \rangle(z)$], and deviations from zonal averages [$\underline{v}'(x, z)$, $\underline{\theta}'(x, z)$]. The section-averaged values are used to derive the barotropic component. The overturning component is estimated from the zonally averaged baroclinic values, whereas the horizontal temperature fluxes can be derived from $\underline{v}'(x, z)$ and $\underline{\theta}'(x, z)$. The barotropic heat fluxes are small, with an average value of 0.01 PW . The time-mean northward overturning heat flux is about 0.55 PW . The horizontal heat fluxes are southward with a mean value of -0.17 PW . Both the mean barotropic and horizontal heat fluxes are consistent with the values estimated from the XBT measurements (Dong et al. 2009). However, the overturning heat flux is relatively weak compared with the value of 0.75 PW from the XBT measurements, which explains the weak MHT.

The time-mean heat transport into the South Atlantic from the Pacific through Drake Passage is about $1.65 \pm 0.09\text{ PW}$. Although the volume transport south of South Africa is slightly larger than that across Drake Passage, the heat transport is smaller, about $1.26 \pm 0.23\text{ PW}$. This smaller eastward heat transport south of South Africa is potentially due to the westward flow of the Agulhas Current, which brings warm water from the Indian Ocean into the South Atlantic. The Ekman transports across

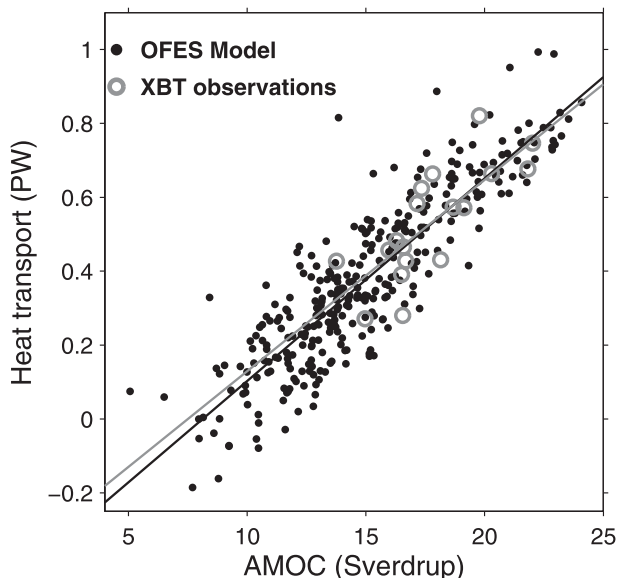


FIG. 5. Scatterplot of the strength of the AMOC vs total MHT across 34°S. Dots and circles correspond to OFES and XBT observations, respectively. The black and gray lines indicate the regression of the heat transport to the AMOC from OFES and XBT observations, respectively.

both choke points are negligible because the wind fields in the Southern Ocean are predominantly westerlies. Hence, the transports across Drake Passage and south of South Africa are mainly from the geostrophic component.

2) THE STRENGTH OF THE AMOC

The strength of the AMOC in OFES at 34°S, defined as the maximum cumulative volume transport from the ocean surface downward, is about 15.0 ± 3.7 Sv on average, which is lower than the mean AMOC of 17.9 ± 2.2 Sv from observations (Dong et al. 2009) but within the error bars. Of this 15-Sv transport, the Ekman component accounts for 2.1 ± 2.5 Sv, which is consistent with the Dong et al. (2009) estimate derived from XBT observations. The geostrophic flow contributes about 12.9 ± 2.1 Sv transport, which is lower than the value of 15.7 ± 2.6 Sv from Dong et al. (2009).

Both the strength of the AMOC and MHT across 34°S from the model are weak compared to those from observations because of the weak geostrophic transport. However, the response of the MHT to the AMOC strength in the model is consistent with observations (Fig. 5). Statistical analysis suggests that a 1-Sv increase in the AMOC would give an increase of MHT of 0.054 ± 0.003 PW in OFES, which is consistent with that derived from XBT observations (Dong et al. 2009). The mean AMOC strength from the model is about 3 Sv lower than that derived from observations; using the AMOC–MHT relationship, this would result in a lower MHT by 0.15 PW. This

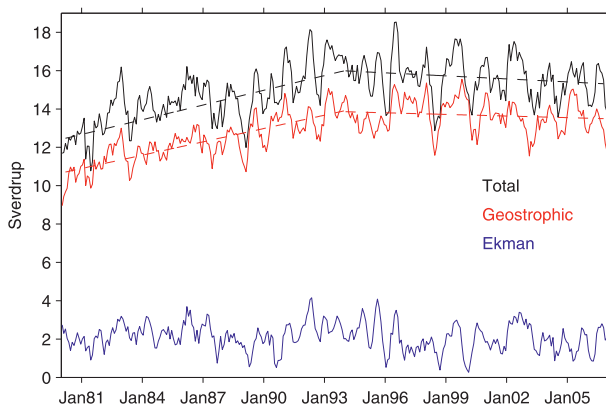


FIG. 6. Time series of the strength of the AMOC (black) at 34°S and contributions from the geostrophic (red) and Ekman (blue) components. Dashed lines denote the linear trends from least squares analysis.

is consistent with the difference of 0.16 PW between model and observed MHT, suggesting that the lower MHT is likely due to the weak AMOC in the model.

b. Temporal variability

In this section, the temporal variations in volume and heat transports across the boundaries of our study region are analyzed. All analyses are based on the monthly averages of the transports. A 3-month running mean was performed on all variables to further reduce noise. Because we are interested in variations on interannual to longer time scales, the seasonal cycles estimated from a least squares annual harmonic analysis have been removed from all variables. Correlation coefficients are computed among variables before and after removing the linear trend from the entire time series of each variable. The correlation coefficients derived from detrended time series are given in parentheses, unless otherwise specified. We note that the significance of correlations in our analysis is relative to the 95% significance level of 0.3. This significance level is determined with the assumption that the decorrelation scale in the variables is 8 months, which is based on the first zero crossing of the autocorrelation. Thus, the number of degrees of freedom is assumed to be 40.

1) THE AMOC STRENGTH AT 34°S

The strength of the AMOC at 34°S from the 27-yr period varies from 10.7 to 18.5 Sv (Fig. 6). The main feature in the AMOC temporal variation is its strengthening during the first half of our study period: that is, from 1980 to 1993. The AMOC strength fluctuates around its mean value after 1993, though it decreases slightly. Statistical analysis for the first 14-yr period (1980–93) gives an increasing trend of 2.5 ± 0.4 Sv decade⁻¹, which is significant at the 95% significance level. The second

half of our study period shows a marginal decreasing trend of -0.6 ± 0.4 Sv decade $^{-1}$. We note that the separation point 1993 is chosen subjectively to maximize the increasing and decreasing linear trends. However, no statistically significant difference was found if the separation point is shifted by ± 1 yr. This is also true for the analyses presented later in this study.

Also shown in Fig. 6 are the contributions of the geostrophic and Ekman transports to the AMOC strength. The geostrophic component accounts for 75% of the total variance of the AMOC and is highly correlated to the AMOC with a correlation coefficient of 0.86 (0.81). In particular, Fig. 6 suggests that the strengthening of the AMOC from 1980 to 1993 is solely due to the geostrophic component, which is confirmed by the linear trend of 2.4 ± 0.3 Sv decade $^{-1}$ in geostrophic transport. About 25% of the total variance in the AMOC is explained by the Ekman transport. However, no statistically significant linear trends were found in the Ekman contribution (Fig. 6) for both the first and second half of the time series. Statistical analysis gives a correlation coefficient of 0.49 (0.67) between the Ekman component and the AMOC strength, which is relatively lower compared to the geostrophic component but still exceeds the 95% significance level of 0.3.

To examine whether the strengthening of the AMOC comes from boundary currents, we separate the volume transport into three regions (Fig. 7a): the western boundary (west of where current changes from southward to northward, normally around 48°W), the eastern boundary (east of Walvis Ridge, $\sim 3^\circ$ E), and the interior between 48°W and 3°E. The results presented here are not particularly sensitive to these definitions as long as the boundaries are offshore of the boundary currents themselves. The transport in each region is integrated from surface to the depth where the total maximum cumulative transport is located. Only the contributions from the interior region show a marginally significant correlation of 0.34 with the AMOC before the linear trends are removed. However, no statistically significant correlation with the AMOC was found for all three regions after removing the linear trends. The sum of transports from the western boundary and interior significantly correlates with the AMOC both before (0.47) and after (0.42) removing the linear trend, whereas the sum of transports from the eastern boundary and interior only show a significant correlation of 0.42 with AMOC before the linear trend is removed. This statistical analysis suggests that it is important to monitor all three regions to capture the AMOC variability; however, the western and interior regions play a leading role.

The southward transport in the western boundary has strengthened between 1980 and 1993 (Fig. 7a), which

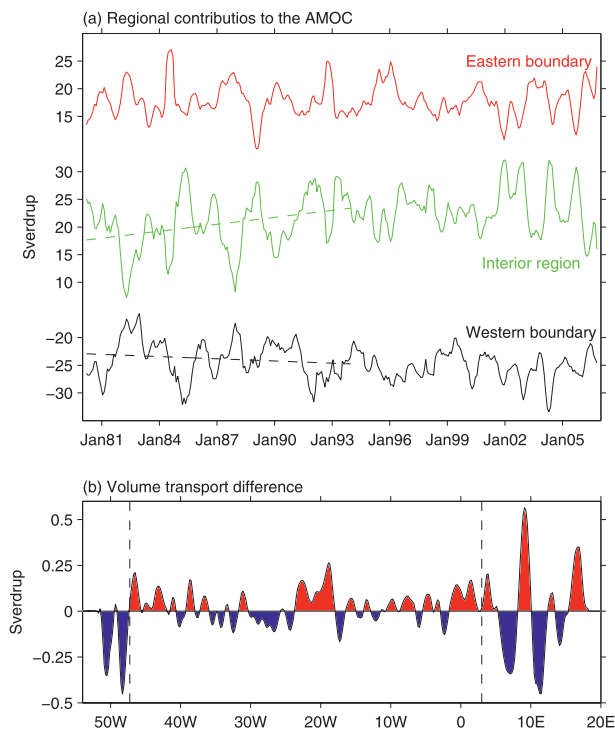


FIG. 7. (a) Regional contributions to the AMOC across 34°S: the eastern (red) and western (black) boundaries and ocean interior region (green). Dashed lines show the linear trend during 1980–93. (b) Zonal distribution of the differences in vertically integrated volume transport between two 10-yr periods: 1994–2003 minus 1980–99. Dashed lines approximate the longitudes where the boundary currents and ocean interior are separated.

should weaken the AMOC. The northward flow in the eastern boundary does not show a statistically significant trend during the period 1980–93 (Fig. 7a). Thus, the strengthening of the AMOC from 1980 to 1993 cannot be explained by the changes in the boundary currents. The only candidate left for the increase in AMOC is the interior region. Indeed, the northward transport in the interior region has increased between 1980 and 1993 (Fig. 7a), with an increase rate of 4.1 ± 1.0 Sv decade $^{-1}$. Part of the increase in the northward interior flow is compensated by the increase in the southward western boundary transport. The dominance of the interior region in the strengthening of the AMOC can be seen from the zonal distribution of the differences in vertically integrated volume transport between two 10-yr averages (1994–2003 minus 1980–89; Fig. 7b). Figure 7b clearly shows the increase in both the southward flow in the western boundary and the northward flow in the interior region. Again, our analyses of OFES suggest that it is important to monitor the ocean interior as well as the boundary currents to capture the AMOC variability, which is consistent with the results from XBT measurements (Dong et al. 2009).

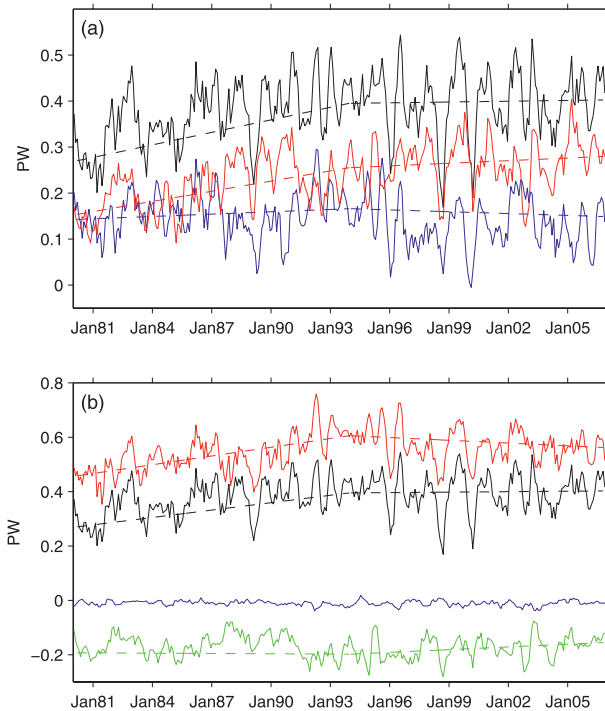


FIG. 8. Time series of the MHT (black) across 34°S and contributions (a) from the geostrophic (red) and Ekman (blue) components and (b) from the barotropic (blue), overturning (red), and horizontal (green) components. Dashed lines are the corresponding linear trends from least squares analysis.

2) MERIDIONAL HEAT TRANSPORT ACROSS 34°S

The net meridional heat transport across 34°S varies in the range of 0.17–0.54 PW during our study period (Fig. 8a). It is not surprising from the close correspondence between the strength of the AMOC and the MHT (Fig. 5) that the variations in MHT are very similar to the variations in the AMOC (Fig. 6). In particular, the net heat transport also shows an increase from 1980 to 1993. The least squares fit analysis for the first 14-yr period suggests that the MHT increases with a rate of $0.09 \pm 0.02 \text{ PW decade}^{-1}$. Although the heat transport experiences relatively large fluctuation after 1993, no statistically significant linear trend was found.

Both changes in the strength of the AMOC and temperature differences between the northward and southward flow water can induce changes in the MHT. To estimate the contributions of the changes in the AMOC strength and temperature fields, we separate the velocity and temperature into time mean $[\bar{v}(x, z), \bar{T}(x, z)]$ and deviations from their time mean $[v'(x, z, t), T'(x, z, t)]$. The contributions from changes in the AMOC and temperature are computed from $v'(x, z, t)\bar{T}(x, z)$ and $\bar{v}(x, z)T'(x, z, t)$, respectively. Our examination indicates that the increase in the MHT during 1980–93 is mainly due to the changes

in velocity field: that is, due to the strengthening of the AMOC itself. In general, ocean temperature has increased during our study period, possibly related to the changes in the AMOC. However, the warming trends in the deep ocean is stronger than that in the upper water column, which suggests that the long-term changes in temperature between the northward and southward flows associated with mean AMOC would decrease the MHT, counteracting the effect from the strengthening of the AMOC.

Variations in the regional contributions (not shown) to the MHT are very similar to their contributions to the AMOC. No significant correlations with the net heat transport were found for all three regions, suggesting that there is no dominant contribution to the relatively high-frequency changes in the MHT across 34°S . Similar to the regional contributions to the AMOC, the increase in the MHT during 1980–93 appears to be due to the interior region, which increases with a rate of $0.18 \pm 0.06 \text{ PW decade}^{-1}$. The southward heat transport at the western boundary also experiences an increasing trend of $0.09 \pm 0.05 \text{ PW decade}^{-1}$. This increase in southward heat transport is more than compensated by the increased MHT in the interior region. No significant linear trend was found for the MHT at the eastern boundary.

Similar to the AMOC strength, the geostrophic component is the largest contributor to the long-term changes in the MHT (Fig. 8a); it accounts for 60% of the total variance in the MHT, lower than its 75% contribution to the AMOC variability. The Ekman transport (Fig. 8a) accounts for 40% of the total variance in the MHT. This large contribution to heat transport from the Ekman component, compared to its 25% contribution to the AMOC variability, can be explained by the higher temperature at the ocean surface. However, the geostrophic transport is the major contributor to the linear increase in MHT during 1980–93 (Fig. 8a). Statistical analysis of the geostrophic heat transport gives a linear increasing trend of $0.08 \pm 0.02 \text{ PW decade}^{-1}$. The Ekman transport during 1980–93 also experiences an increasing trend of $0.02 \pm 0.02 \text{ PW decade}^{-1}$; however, it is not statistically significant. Both the geostrophic and Ekman heat transports show a marginal linear trend during the second half of our study period (1994–2006), with an increasing trend of $0.02 \pm 0.02 \text{ PW decade}^{-1}$ in the geostrophic component and a decreasing trend of $-0.02 \pm 0.02 \text{ PW decade}^{-1}$ in the Ekman component.

The separation of the MHT into the barotropic, overturning, and horizontal heat fluxes suggests that the overturning component is the major contributor to the variations in the MHT on interannual to longer time scales (Fig. 8b). Similar to its mean value, variability in the barotropic heat transport is negligible. The overturning heat transport accounts for 78% of the total variance of

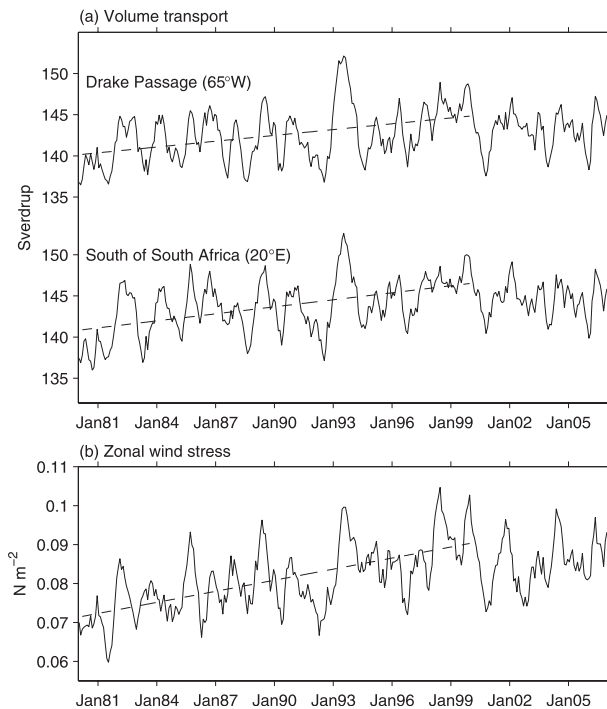


FIG. 9. Time series of (a) volume transports across Drake Passage and south of South Africa and (b) spatially averaged zonal wind stress in the Southern Ocean (30° – 75° S, 180° – 180°). The corresponding linear trends are shown as dashed lines.

MHT, and they are highly correlated with a correlation coefficient of 0.80 (0.78). The remaining 22% of the total variance is set by the horizontal component, which is also correlated with the MHT at the 95% significance level, with a correlation coefficient of 0.41 (0.45). The increase in the MHT during the first 14 yr is a result of the increasing overturning heat transport; it increases at a rate of 0.10 ± 0.02 PW decade⁻¹. No statistically significant linear trends were found in the horizontal heat transport during 1980–93. The overturning and horizontal components experience an equal but opposite linear trend of 0.03 ± 0.02 PW decade⁻¹ during 1994–2006, with a decreasing trend in the overturning component and an increasing trend in the horizontal component.

3) VOLUME TRANSPORT ACROSS DRAKE PASSAGE AND SOUTH OF SOUTH AFRICA

As expected from volume conservation in the box and the nearly zero volume transport across 34° S, the volume transports across Drake Passage and south of South Africa are nearly identical and are highly correlated with a correlation coefficient of 0.93 (0.92) (Fig. 9a). Similar to the total transports across 34° S, the volume transports across both choke points also experience statistically significant increasing trends, suggesting that the ACC has strengthened during our study period. However,

unlike at 34° S, where the increase in transports occur during the 14 yr, the volume transports across both choke points show increase during a 20-yr period from 1980 to 1999. The eastward transport across Drake Passage increases at a rate of 2.4 ± 0.5 Sv decade⁻¹ during 1980–99. The transport south of South Africa experiences a slightly stronger increasing trend of 2.9 ± 0.5 Sv decade⁻¹ but is not statistically different from that across Drake Passage. The volume transports across both choke points fluctuate around their mean values after 1999.

One possible explanation for the strengthening of the ACC is the changes in the wind field. The ACC is largely driven by the Southern Hemisphere westerly winds, which have strengthened and shifted southward in recent decades (e.g., Thompson and Solomon 2002; Marshall 2003). A number of studies (e.g., Hallberg and Gnanadesikan 2001; Hogg and Blundell 2006; Hogg et al. 2008) argued that, for stronger winds, the ACC is in an eddy-dominated regime where changes in the wind stress induce little change in ACC transport. Whether the ACC has reached its “eddy saturation” regime is still in debate, and it is out of scope of current study. However, the peak of ACC transport in 1998–99 in OFES is consistent with the results of Meredith et al. (2004), who found that the ACC transport peaked in 1998 from Antarctic sea level measurements, the same period when the Southern Ocean wind reached its maximum strength. Thus, the upward trend in the ACC transport is likely a response of the Southern Ocean to the observed polarward intensification of the westerly winds (e.g., Hall and Visbeck 2002; Sen Gupta and England 2006). The zonal wind stress averaged over the entire Southern Ocean (30° – 75° S, 180° – 180°) (Fig. 9b) demonstrates coherent variations with the volume transports across both choke points. The correlations of the spatially averaged zonal wind stress with the volume transports across Drake Passage and south of South Africa are 0.72 (0.69) and 0.77 (0.70), respectively, exceeding the 95% significance level of 0.3.

4) HEAT TRANSPORT ACROSS DRAKE PASSAGE AND SOUTH OF SOUTH AFRICA

The heat transport across Drake Passage (Fig. 10) varies similarly to the volume transport on interannual time scales. Statistical analysis gives a correlation coefficient of 0.67 (0.62) between volume and heat transports. However, unlike the volume transport, which increases from 1980 to 1999 and fluctuates around its mean value after 1999, the increase in heat transport occurs during the entire 27-yr period. Statistical analysis gives an increasing rate of 0.03 ± 0.01 PW decade⁻¹. As we mentioned earlier, changes in both velocity and temperature fields can induce variations in the heat transport. Dividing the heat transport into contributions from velocity

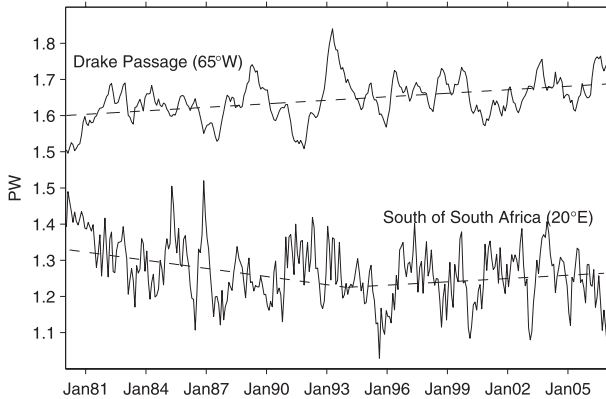


FIG. 10. The net eastward heat transports across (top) Drake Passage and (bottom) south of South Africa. Dashed lines indicate the corresponding linear trends. Units are in PW.

$[v'(x, z, t)\bar{T}(x, z)]$ and temperature $[\bar{v}(x, z)T'(x, z, t)]$ suggests that 65% of the total variance in heat transport across Drake Passage is due to variability in the temperature fields. However, the changes in the velocity field have a large contribution to the long-term linear trend in the total heat transport; they account for 66% of linear increase in the heat transport across Drake Passage during our study period.

Unlike at Drake Passage where the heat transport and volume transport are positively correlated, no statistically significant correlation was found between the volume and heat transports south of South Africa. In particular, opposite to the increase in volume transport between 1980 and 1999 south of South Africa, the heat transport shows a statistically significant decreasing trend during 1980–93, with a decreasing rate of -0.08 ± 0.02 PW decade⁻¹ (Fig. 10). This decrease in eastward heat transport south of South Africa can be understood as an increase in westward heat transport: that is, an increase in heat transport from Indian Ocean to the South Atlantic.

As shown in Fig. 2, different from the ACC-dominant eastward flow at Drake Passage, the transport south of South Africa is controlled by two current systems: the ACC and Agulhas Current system. The Agulhas Current system includes the westward-flowing Agulhas Current and its return flow. It has been a difficult task to separate the Agulhas return flow from the ACC because of its mixture with the Subantarctic Front (van Sebille et al. 2010). Because our focus is on heat transport, for simplicity we define the Agulhas leakage as the total heat transport from South Africa coast to the location where the meridional cumulative volume transport reaches zero. This potentially gives a lower bound estimate of the Agulhas leakage because this neglects the transport of rings and any portion of the upper limb of the MOC from the Indian Ocean. Our definition gives a time-mean

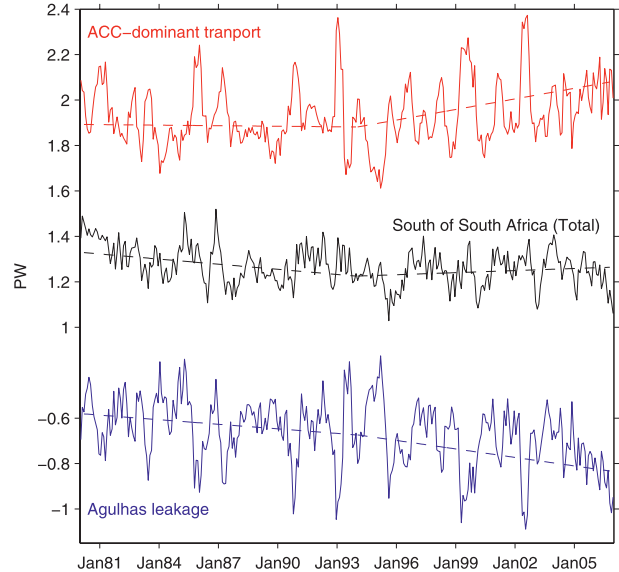


FIG. 11. Time series of the total eastward heat transport (black) across south of South Africa and its separation of the westward Agulhas leakage (blue) and the ACC-dominant eastward heat transport (red). The corresponding linear trend in each variable is shown as a dashed line.

Agulhas leakage of -0.67 ± 0.32 PW (Fig. 11). In terms of long-term variability, we found that the heat transport associated with the westward Agulhas leakage has been increasing during our entire study period, with a rate of -0.07 ± 0.02 PW decade⁻¹ (Fig. 11). The ACC-dominant eastward flow does not show a statistically significant linear trend during the first half of our study period (1980–93). However, it experiences a strong increase during 1994–2006 (Fig. 11). Statistical analysis gives an increasing rate of 0.15 ± 0.06 PW decade⁻¹ for the second half of our study period.

c. What controls the long-term change in meridional heat transport across 34°S?

Our statistical analyses indicate that the MHT across 34°S has increased during the first half of our study period: that is, 1980–93. The question is, where does this increased heat advected to the north in the South Atlantic come from? There are three sources for the MHT: heat storage rate in our study region $\partial hc/\partial t$, heat gain from the atmosphere Q_{net} , and heat convergence through interocean exchanges. The interocean exchanges include transport from the Pacific through Drake Passage HT_{Drake} and that from the Indian Ocean through south of South Africa HT_{Africa} . The heat transport across 34°S $HT_{34^\circ\text{S}}$ can be expressed as

$$HT_{34^\circ\text{S}} = \frac{\partial hc}{\partial t} + Q_{\text{net}} + (HT_{\text{Drake}} - HT_{\text{Africa}}). \quad (1)$$

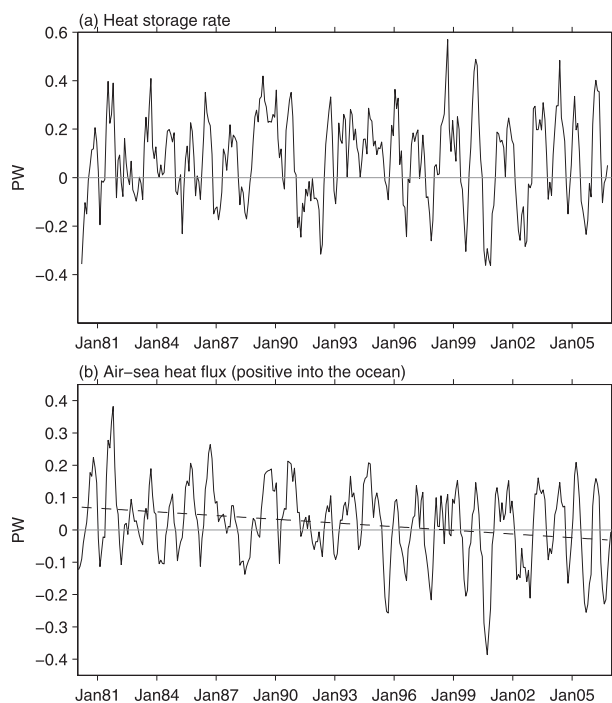


FIG. 12. Anomalies of (a) time rate of change of heat content (i.e., heat storage rate) and (b) air-sea heat fluxes (positive into the ocean) integrated in our study region. Dashed line shows the linear trend from least squares fit. Units are in PW.

Our analyses in section 3b indicate that HT_{Drake} has an increasing trend and that HT_{Africa} has a decreasing trend during the period 1980–93, when $HT_{34^{\circ}\text{S}}$ shows an increasing trend. Thus, the transports across the two choke points give an increase in heat convergence into the South Atlantic, with an increasing rate of 0.12 ± 0.04 PW decade⁻¹ for the period 1980–93. This suggests that both HT_{Drake} and HT_{Africa} are potential causes for the increase in the MHT. We note that the increasing rate in the heat transport across Drake Passage during 1980–93 is about 0.04 PW decade⁻¹, slightly larger than its increasing trend of 0.03 PW decade⁻¹ during our entire study period. Our separation of HT_{Africa} into the ACC-dominant eastward transport and the westward Agulhas leakage suggested that the decrease in the eastward heat transport across south of South Africa is due to the increase in westward Agulhas leakage, not the decrease in the ACC-dominant eastward heat transport.

Although the total heat content in our study region has been increasing during the 27-yr period (not shown), the time derivative of the heat content (i.e., heat storage rate $\partial hc/\partial t$) has no statistically significant long-term trend for the period 1980–93 as well as for the entire time series (Fig. 12a). This eliminates the possibility that the heat storage rate contributes to the increase in the MHT. The air-sea heat flux (positive into the ocean) from OFES

shows a decreasing trend of 0.03 ± 0.01 PW decade⁻¹ for the entire period (Fig. 12b), suggesting that the heat input into the ocean from the atmosphere has decreased since 1980. This eliminates the air-sea heat flux as a candidate for the increase in the MHT.

Thus, the answer to the question posed at the beginning of this section is that the possible explanation for the increase in the MHT across 34°S is the heat convergence through interocean exchanges. Part of the increased heat transported into the South Atlantic from the Pacific and Indian Oceans is released to the atmosphere through air-sea heat exchange. Although there is no question that the Agulhas Current system has large contributions to the increase in heat convergence into the South Atlantic and the increasing rate in the westward Agulhas leakage and that in the MHT across 34°S are not statistically different, we cannot rule out the role of the ACC transport through Drake Passage. Detailed analysis on water mass classes is needed to quantify the role of transports from the Pacific and Indian Oceans in the MHT, which is out of the scope of current study.

4. Discussion and conclusions

The analysis of OFES for the period 1980–2006 in the South Atlantic indicates that both the strength of the AMOC and the MHT across 34°S are weaker on average than those derived from observations. However, OFES gives the same response of the MHT to the changes in the AMOC strength: a 1-Sv increase in the AMOC strength would cause a 0.054 ± 0.003 PW increase in the MHT at 34°S . OFES suggests an increase in both the AMOC strength and the MHT across 34°S from 1980 to 1993, which is dominated by the ocean interior region between 48°W and 3°E . However, both the boundary currents and the interior region are important in explaining the interannual to decadal variations in the AMOC and in the MHT, suggesting that it is important to monitor the ocean interior region as well as boundary currents in order to capture the variability in the AMOC and the MHT. Separating the total transports across 34°S into geostrophic and Ekman components suggests that the changes in total transports on a decadal time scale are mainly set by the geostrophic transports.

There are three candidates for the increase in the MHT: heat storage rate, heat gain from the atmosphere, and heat convergence through interocean exchanges with the Pacific and Indian Oceans. Our analysis suggests that the heat convergence through interocean exchanges is the only contributor to the increase in the MHT across 34°S , suggesting the importance in understanding the interocean exchanges in the South Atlantic for long-term

climate change. The linear increase in heat input into the South Atlantic from the Indian Ocean between 1980 and 1993 is twice as large as that from the Pacific. About 25% of the increased heat convergence is released to the atmosphere. We note that conclusions drawn from this study are based on OFES. No sufficient observations are currently available to examine the realism of those conclusions. An international program for observing the South Atlantic MOC is currently proposed, which will provide valuable data to advance our knowledge of the inter-ocean exchanges and to evaluate models.

Changes in the AMOC have been linked to changes in the deep convection in the subpolar North Atlantic and changes in the Southern Ocean wind. The increase in AMOC at 34°S from 1980 to 1993 is incoherent with the strengthening of the Southern Ocean wind from 1980 to 1999, which does not support the idea that the Southern Ocean winds force the strengthening of the AMOC. The southward transport in the western boundary at 34°S has strengthened during 1980–93; in particular, the deep western boundary current shows an increasing trend of 3.1 ± 0.5 Sv decade⁻¹ (not shown), suggesting that the increase of the AMOC in OFES may be related to the strengthening of the deep western boundary current. It should be noted that the realism of these conclusions drawn from OFES depends on how well the Southern Ocean dynamics are reproduced in the model, particularly the dynamics of the water mass formation and transformation processes. Further detailed studies are needed to assess the model's ability in representing the Southern Ocean dynamics and to understand the AMOC variability and its mechanism in OFES.

Interocean exchanges in the South Atlantic have been the focus of numerous studies because of their potential link to the AMOC, though the relative contributions of the cold- and warm-water routes on the source of the northward-flowing water in the upper branch of the AMOC is still under debate. Our analysis suggests that both the cold-water route from the Pacific and warm-water route from the Indian Ocean play a role in the long-term changes in the MHT, but the warm-water route plays a more important role during the 1980–93 period. However, this conclusion is drawn from the section-integrated heat transports, which do not provide information on the variability of interocean exchanges of various water masses and their northward transport in the South Atlantic. The inflow of water from Pacific in certain density classes (e.g., the Antarctic Intermediate Water) may play an important role in the northward transport of those water masses, which could influence the strength of the AMOC (e.g., Rintoul 1991; Saenko et al. 2003). Detailed examination of interocean exchanges in density classes needs to be conducted to examine water mass transformation within the South

Atlantic and to assess their possible influence in variations in the AMOC strength.

The increase in Agulhas leakage in OFES is consistent with results from recent studies (Bjastoch et al. 2009; Rouault et al. 2009; van Sebille et al. 2009), though it is still in debate what causes the increased leakage. Bjastoch et al. (2009) attributed the increase to the southward movement of the ocean current system associated with the poleward shift of the Southern Hemisphere westerly winds. Rouault et al. (2009) suggested that the increase in the Agulhas leakage is due to the strengthening of the Agulhas Current forced by wind stress curl. We note that the Agulhas leakage defined in this study in terms of heat transport is different from the traditional definition of Agulhas leakage, which is the amount of water in the Agulhas Current system that ends up in the Atlantic Ocean. Estimating the magnitude of this traditional definition of Agulhas leakage is extremely difficult because of the complexity of currents and intense mixing in the vicinity of Agulhas retroflexion (e.g., van Sebille 2009). Dedicated effort is needed to accurately quantify the magnitude of Agulhas leakage, and it is out of the scope of current study. Our simplified definition of heat transport from Agulhas leakage, the integrated temperature flux from South Africa coast to the location where the cumulative volume transport reaches zero, likely gives a lower bound of leakage of temperature flux from Indian Ocean to the South Atlantic from the Agulhas Current system. Nevertheless, OFES suggests that the Agulhas Current system plays an important role in the MHT in the South Atlantic.

Acknowledgments. The authors thank Dr. Wilbert Weijer and the other anonymous reviewer for their valuable comments and suggestions. OFES outputs are from the Japanese Earth Simulator Center (JAMSTEC). This work is supported by NOAA Grant NA10OAR4310206 and the base funding of the NOAA/Atlantic Oceanographic and Meteorological Laboratory (AOML).

REFERENCES

- Baringer, O. M., and S. L. Garzoli, 2007: Meridional heat transport determined with expendable bathythermographs. Part I: Error estimates from model and hydrographic data. *Deep-Sea Res. I*, **54**, 1390–1401.
- Bjastoch, A., C. W. Boning, and J. R. E. Lutjeharms, 2008: Agulhas leakage dynamics affects decadal variability in Atlantic overturning circulation. *Nature*, **27**, 489–492.
- , —, F. U. Schwarzkopf, and J. R. E. Lutjeharms, 2009: Increase in Agulhas leakage due to poleward shift of Southern Hemisphere westerlies. *Nature*, **462**, 495–498.
- Broecker, W. S., 1991: The great ocean conveyor. *Oceanography*, **4**, 79–89.

- , 1997: Thermohaline circulation, the Achilles heel of our climate system: Will man-mode CO₂ upset the current balance? *Science*, **278**, 1582–1588.
- Bryden, H. L., and S. Imawaki, 2001: Ocean heat transport. *Ocean Circulation and Climate*, G. Siedler, J. Church, and J. Gould, Eds., Academic Press, 455–474.
- Cunningham, S. A., S. G. Alderson, B. A. King, and M. A. Brandon, 2003: Transport and variability of the Antarctic Circumpolar Current in Drake Passage. *J. Geophys. Res.*, **108**, 8084, doi:10.1029/2001JC001147.
- , and Coauthors, 2007: Temporal variability of the Atlantic meridional overturning circulation at 26.5°N. *Science*, **312**, 935–938.
- , and Coauthors, 2010: The present and future system for measuring the Atlantic meridional overturning circulation and heat transport. *Proc. OceanObs'09: Sustained Ocean Observations and Information for Society Conf.*, Vol. 2, Venice, Italy, ESA, WPP-306.
- Dong, S., S. Garzoli, M. Baringer, C. Meinen, and G. Goni, 2009: Interannual variations in the Atlantic meridional overturning circulation and its relationship with the net northward heat transport in the South Atlantic. *Geophys. Res. Lett.*, **36**, L20606, doi:10.1029/2009GL039356.
- Ganachaud, A., and C. Wunsch, 2000: Improved estimates of global ocean circulation, heat transport and mixing from hydrographic data. *Nature*, **408**, 453–457.
- Garzoli, S. L., and A. L. Gordon, 1996: Origins and variability of the Benguela Current. *J. Geophys. Res.*, **101**, 897–906.
- , and M. O. Baringer, 2007: Meridional heat transport determined with expandable bathythermographs—Part II: South Atlantic transport. *Deep-Sea Res. I*, **54**, 1402–1420.
- , and R. Matano, 2011: The South Atlantic and the Atlantic meridional overturning circulation. *Deep-Sea Res. II*, doi:10.1016/j.dsr2.2010.10.063, in press.
- Gordon, A. L., 1985: Indian-Atlantic transfer of thermocline water at the Agulhas retroflection. *Science*, **227**, 1030–1033.
- Gregory, J. M., and Coauthors, 2005: A model intercomparison of changes in the Atlantic thermohaline circulation in response to increasing atmosphere CO₂ concentration. *Geophys. Res. Lett.*, **32**, L12703, doi:10.1029/2005GL023209.
- Hall, A., and M. Visbeck, 2002: Synchronous variability in the Southern Hemisphere atmosphere, sea ice, and ocean resulting from the annular mode. *J. Climate*, **15**, 3043–3057.
- Hallberg, R., and A. Gnanadesikan, 2001: An exploration of the role of transient eddies in determining the transport of a zonally reentrant current. *J. Phys. Oceanogr.*, **31**, 3312–3330.
- Hogg, A. M., and J. R. Blundell, 2006: Interdecadal variability of the Southern Ocean. *J. Phys. Oceanogr.*, **36**, 1626–1645.
- , M. P. Meredith, J. R. Blundell, and C. Wilson, 2008: Eddy heat flux in the Southern Ocean: Response to variable wind forcing. *J. Climate*, **21**, 608–620.
- Lumpkin, R., and K. Speer, 2007: Global ocean meridional overturning. *J. Phys. Oceanogr.*, **37**, 2550–2562.
- Marsh, R., W. Hazeleger, A. Yool, and E. J. Rohling, 2007: Stability of the thermohaline circulation under millennial CO₂ forcing and two alternative controls on Atlantic salinity. *Geophys. Res. Lett.*, **34**, L03605, doi:10.1029/2006GL027815.
- Marshall, G. J., 2003: Trends in the southern annular mode from observations and reanalyses. *J. Climate*, **16**, 4134–4143.
- Maximenko, N. A., B. Bang, and H. Sasaki, 2005: Observational evidence of alternating zonal jets in the world ocean. *Geophys. Res. Lett.*, **32**, L12607, doi:10.1029/2005GL022728.
- Meredith, M. P., P. L. Woodworth, C. W. Hughes, and V. Stepanov, 2004: Changes in the ocean transport through Drake Passage during the 1980s and 1990s, forced by changes in the Southern Annual Mode. *Geophys. Res. Lett.*, **31**, L21305, doi:10.1029/2004GL021169.
- Nonaka, M., H. Nakamura, Y. Tanimoto, T. Kagimoto, and H. Sasaki, 2006: Decadal variability in the Kuroshio–Oyashio Extension simulated in an eddy-resolving OGCM. *J. Climate*, **19**, 1970–1989.
- Pacanowski, R. C., and S. M. Griffies, 1999: MOM 3.0 manual. NOAA/Geophysical Fluid Dynamics Laboratory Tech. Rep. 4, 680 pp.
- Perez, R. C., S. L. Garzoli, C. S. Meinen, and R. P. Matano, 2011: Geostrophic velocity measurement techniques for the meridional overturning circulation and meridional heat transport in the South Atlantic. *J. Atmos. Oceanic Technol.*, in press.
- Rintoul, S. R., 1991: South Atlantic interbasin exchange. *J. Geophys. Res.*, **96**, 2675–2692.
- Rio, M.-H., and F. Hernandez, 2004: A mean dynamic topography computed over the world ocean from altimetry, in situ measurements, and a geoid model. *J. Geophys. Res.*, **109**, C12032, doi:10.1029/2003JC002226.
- Rouault, M., P. Penven, and B. Pohl, 2009: Warming in the Agulhas Current system since the 1980's. *Geophys. Res. Lett.*, **36**, L12602, doi:10.1029/2009GL037987.
- Saenko, O. A., A. J. Weaver, and J. M. Gregory, 2003: On the link between the two modes of the ocean thermohaline circulation and the formation of global-scale water masses. *J. Climate*, **16**, 2797–2801.
- Sarmiento, J. L., 2004: High-latitude controls of thermocline nutrients and low biological productivity. *Nature*, **427**, 56–60.
- Sasaki, H., M. Nonaka, Y. Masumoto, Y. Sasai, H. Uehara, and H. Sakuma, 2007: An eddy-resolving hindcast simulation of the quasi-global ocean from 1950 to 2003 on the Earth Simulator. *High Resolution Numerical Modelling of the Atmosphere and Ocean*, K. Hamilton and W. Ohfuchi, Eds., Springer, 157–185.
- Saunders, P. M., and B. A. King, 1995: Oceanic fluxes on the WOCE A11 section. *J. Phys. Oceanogr.*, **25**, 1942–1958.
- Sen Gupta, A., and M. England, 2006: Coupled ocean–atmosphere–ice response to variations in the southern annular mode. *J. Climate*, **19**, 4457–4486.
- Sloyan, B. M., and S. R. Rintoul, 2001: The Southern Ocean limb of the global deep overturning circulation. *J. Phys. Oceanogr.*, **31**, 143–173.
- Stocker, T. F., and A. Schmittner, 1997: Influence of CO₂ emission rates on the stability of the thermohaline circulation. *Nature*, **388**, 862–865.
- Taguchi, B., S.-P. Xie, N. Schneider, M. Nonaka, H. Sasaki, and Y. Sasai, 2007: Decadal variability of the Kuroshio Extension: Observations and an eddy-resolving model hindcast. *J. Climate*, **20**, 2357–2377.
- Talley, L. D., 2003: Shallow, intermediate and deep overturning components of the global heat budget. *J. Phys. Oceanogr.*, **33**, 530–560.
- Thompson, D., and S. Solomon, 2002: Interpretation of recent Southern Hemisphere climate change. *Science*, **296**, 895–899.
- van Sebille, E., 2009: Assessing Agulhas leakage. Ph.D. thesis, Utrecht University, 166 pp.
- , A. Biastoch, P. J. van Leeuwen, and W. P. M. de Ruijter, 2009: A weaker Agulhas Current leads to more Agulhas

- leakage. *Geophys. Res. Lett.*, **36**, L03601, doi:10.1029/2008GL036614.
- , P. J. Van Leeuwen, A. Biastoch, and W. P. M. De Ruijter, 2010: Flux comparison of Eulerian and Lagrangian estimates of Agulhas leakage: A case study using a numerical model. *Deep-Sea Res. I*, **57**, 319–327.
- von Storch, J.-S., H. Sasaki, and J. Marotzke, 2007: Wind-generated power input to the deep ocean: An estimate using a $1/10^\circ$ general circulation model. *J. Phys. Oceanogr.*, **37**, 657–672.
- Weijer, W., W. P. M. de Ruijter, H. A. Dijkstra, and P. J. van Leeuwen, 1999: Impact of interbasin exchange on the Atlantic overturning circulation. *J. Phys. Oceanogr.*, **29**, 2266–2284.
- , —, A. Sterl, and S. S. Drijfhout, 2002: Response of the Atlantic overturning circulation to South Atlantic sources of buoyancy. *Global Planet. Change*, **34**, 293–311.
- Whitworth, T., III, W. D. Nowlin Jr., and S. J. Worley, 1982: The net transport of the Antarctic Circumpolar Current through Drake Passage. *J. Phys. Oceanogr.*, **12**, 960–971.